Chandra's First Decade of Discovery: Stellar Spectroscopy − Poster 2.8

The X−ray Variability of Capella

Jennifer Posson−Brown, Vinay Kashyap (SAO)

We analyze a decade of Chandra/HRC grating and imaging observations of the active binary Capella to characterize its X-ray variability at various timescales. Examining 205 ks of HRC-I imaging data taken over a time period of 14 months (Dec 2005 to Jan 2007), we find broadband variability at the 2-7% level at short timescales (∼5 ks). At timescales of months to years, we see variations of up to ∼10% in the HRC-I fluxes. Twelve HRC-S/LETG observations taken over the ten year period since launch, for a total of 408 ks, indicate that the overall flux was steady until late 2004 but has increased by roughly 50% since that time.

In addition to monitoring broadband flux, we use the HRC-S/LETG observations to analyze the line emission in detail for several lines. After correcting for the overall flux changes, we determine how the line fluxes vary, allowing us to characterize the variability at different temperatures in the coronae.

Variability is present at all temperatures, and we find that the high temperature plasma is more strongly variable than the low temperature plasma. We explore this variability for spectral lines of different elements at different temperatures. The emission measure structure of Capella undergoes changes more extensive than hitherto suspected.

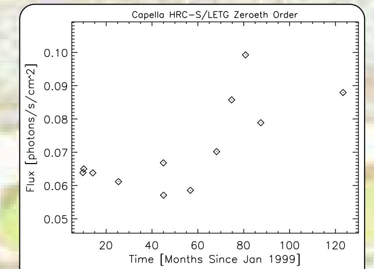

Figure 1 Capella broadband X-ray intensity: zeroeth order flux (corrected by QE uniformity) versus time. Note the rapid increase around 70 months (Fall 2004).

HRC−S/LETG:
Long−term broadband and line flux variability

- Observations listed in Table 1
- Overall luminosity of Capella rapidly increased in late 2004, rising by ∼50% (Figure 1)
- We examine line fluxes for 29 lines, before and after correcting for the broadband flux changes. Fluxes versus time are shown for eight lines in Figure 2.
- After correcting for broadband luminosity changes, we find line flux variability in excess of statistical expectations (Figure 3). We find strong evidence for variability at many temperatures, with dominant contributions between T_{eff}=6.3-6.7.
- We also calculate the fractional variability for the corrected line fluxes (Figure 4). Both cool and hot lines show intrinsic variability.
- There appears to be very little variability at T_{eff}=6.8.

ObsID	Date	Exposure Time s	Y Offset arcmin
1420	1999-10-29	29948.3	0
1248	1999-11-09	84564.4	0
58	2000-03-08	33888.5	0
1009	2001-02-14	26825.4	0
2582	2002-10-04	28657.1	-1.5
3479	2002-10-06	29961.3	1.5
3675	2003-09-28	26965.6	0
5041	2004-09-11	28670.1	3.0
5956	2005-03-31	29928.8	0
6165	2005-10-02	28939.1	-3.0
6472	2006-04-23	29910.4	1.5
10600	2009-04-22	29591.3	-1.5

Table 1 HRC-S/LETG observations of Capella used in this analysis.

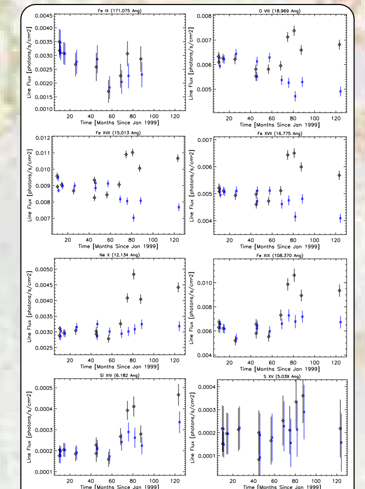

Figure 2 Line fluxes versus time for FeIX (171.075 Å, T_{eff}=5.9), OVIII (18.969 Å, T_{eff}=6.4), FeXVII (15.013 Å, T_{eff}=6.7), FeXVII (16.775 Å, T_{eff}=6.7), NeX (12.134 Å, T_{eff}=6.7), FeXIX (108.37 Å, T_{eff}=6.9), SiXIV (6.182 Å, T_{eff}=7.1), and SXV (5.0387 Å, T_{eff}=6.9). The line fluxes, shown by black diamonds, were calculated by extracting the positive and negative order counts from a narrow region centered on the theoretical wavelength, subtracting background, correcting by the appropriate ARF, and summing. The blue squares show these line fluxes corrected for the variation in the zeroeth order flux (Figure 1).

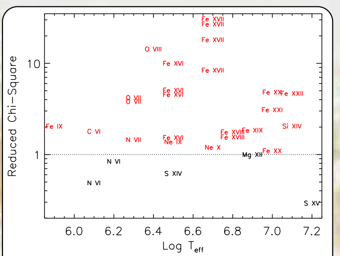

Figure 3 Excess variability in Capella line fluxes at different temperatures. This plot shows reduced chi-square (χ^2_ν), calculated from the line fluxes corrected for zeroeth order variability, versus coronal temperature. We calculate χ^2_ν as $\frac{1}{N}\Sigma\frac{(f-\mu_f)^2}{err_f^2}$ where N is the number of observations, f is the line flux (corrected by zeroeth order), μ_f is the mean line flux, and err_f is the line flux error (statistical). Lines are plotted in black if $\chi^2_\nu < 1$ and red χ^2_ν if > 1.

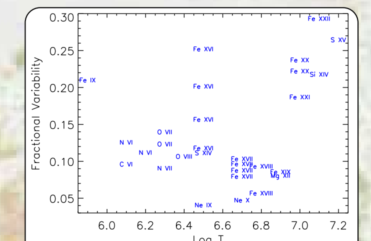

Figure 4 Fractional variability of Capella line fluxes, calculated from line fluxes corrected for broadband luminosity changes, at different temperatures. We calculate fractional variability as $\frac{\sigma_f}{\mu_f}$ where σ_f is the standard deviation of the line fluxes and μ_f is the mean. Hot lines and those at T_{eff}=5.9 and 6.5 show the strongest fractional variability.

HRC−I:
Short−term broadband variability

- Data: 40 observations, approximately 5 ks each (205 ks total) taken at various SIM offsets over Dec 2005 - Jan 2007 (after the rapid luminosity increase seen in Figure 1)
- The combined light curve (Figure 5) shows numerous fluctuations at levels of a few to 10% on timescales of months to years.
- We test whether lightcurve fluctuations are consistent with Poisson noise by computing three overdispersion measures:
  - $\rho_{\rm frac} = \frac{\sigma_J(\delta)}{\sqrt{\mu_J(\delta)}}$
  - $\rho_{\rm diff} = \frac{\sigma_J^2(\delta)-\mu_J(\delta)}{\mu_J(\delta)}$
  - $\rho_{\chi^2} = \sum_{i=1}^{N_\delta} \frac{[C(t_i;J,\delta)^2-\mu_J(\delta)]^2}{N_\delta \mu_J(\delta)}$

  given the counts light curve $C(t_i;J,\delta)$ for ObsID J, where t_i are the N_δ time bins resulting from choosing a bin of size δ, and $\mu_J(\delta)$ and $\sigma_J^2(\delta)$ are the light curve mean and variance. If the lightcurve variations are due to Poisson fluctuations, we expect $\rho_{\rm frac} \approx 1$, $\rho_{\rm diff} \approx 0$, and $\rho_{\chi^2} \approx 1$.
- All three overdispersion measures are greater than expected for most observations (Figure 6), implying significant variability at short timescales (∼ 5 ks).

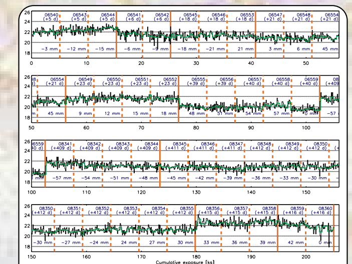

Figure 5 The combined light curve of all HRC-I observations of Capella, spanning 205 ks. The black histogram denotes the count rate for a binning of 100 s, and overlaid on it is the count rate for a binning of 500 s (green histogram). The data gaps between observations are excluded, and indicated by vertical red lines (solid when the gaps are > 100 s, dashed otherwise). The data comprise 40 ObsIDs (noted at the top of each segment, along with the day since 2005-dec-01 that the observation started). The SIM offset at which each observation is carried out is indicated at the bottom of each segment. The counts are corrected by the QE uniformity at each observation location. Count rates vary from ∼20-23 s^{-1}.

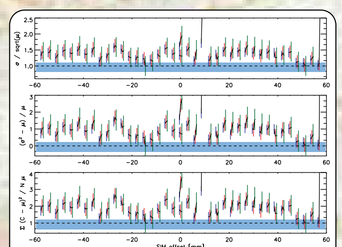

Figure 6 Overdispersion in the light curve in each Capella ObsID. The overdispersion measures $\rho_{\rm frac}$ (top), $\rho_{\rm diff}$ (middle), and ρ_{χ^2} (bottom) are calculated for each ObsID for different values of the light curve bin sizes δ = 25, 50, 100 s, and are denoted by the thin vertical lines grouped around the SIM offset for that observation. The lines are offset from each other for clarity and have δ increasing from left to right, and the measured values for each ObsID are connected by dark lines. The vertical lines represent the $\pm3\sigma$ error bars for the *null*, determined from Monte Carlo simulations of a model without any intrinsic variability but matching the count rate and exposure time of the observation. The values expected for the null model are shown for each $\rho_{(\cdot)}$ as the horizontal dashed line. The overdispersion measures computed for combined HRC-I HZ 43 data (for a binning that matches δ = 25 s for Capella) is shown as the pale blue band whose width corresponds to the $\pm3\sigma$ error bounds determined the same way as for Capella. The HZ 43 overdispersion measures are consistent with no intrinsic variabilty, confirming that the overdispersion detected for Capella is real and not due to QE uniformity uncertainties.

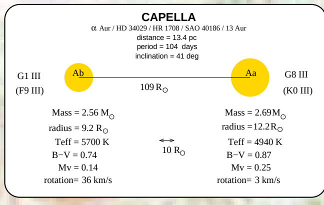

References

- Güdel M 2004, A&ARev, 12, 71
- Johnson O, Drake J J, Kashyap V, Brickhouse N S, Dupree A K, Freeman P, Young P R & Kriss G A 2002, ApJ, 565, 97
- Kashyap V L & Posson-Brown J, submitted to ApJ
- Raassen A J J & Kaastra J S 2007, A&Ap, 461, 679

background image: http://space.mit.edu/CSR/LETG_closeup.gif